



# Validation and implementation of a liquid chromatography/tandem mass spectrometry assay for quantitation of the total and unbound RO4929097, a $\gamma$ -secretase inhibitor targeting Notch signaling, in human plasma

Jianmei Wu, Richard Wiegand, Patricia LoRusso, Jing Li\*

Karmanos Cancer Institute, Wayne State University, Detroit, MI 48201, USA

## ARTICLE INFO

### Article history:

Received 21 October 2010

Accepted 23 March 2011

Available online 31 March 2011

### Keywords:

RO4929097

$\gamma$ -Secretase inhibitor

High performance liquid chromatography

Mass spectrometry

LC-MS/MS

Pharmacokinetics

## ABSTRACT

A reversed-phased liquid chromatography with tandem mass spectrometry (LC-MS/MS) method was developed and validated for quantitation of the total and unbound RO4929097, a  $\gamma$ -secretase inhibitor targeting Notch signaling, in human plasma. Sample preparation involved a liquid–liquid extraction with ethyl acetate. Chromatographic separation was achieved on a Waters X-Terra™ MS C<sub>18</sub> column with an isocratic mobile phase consisting of methanol/0.45% formic acid in water (60:40, v/v) running at a flow rate of 0.2 ml/min for 6 min. The lower limits of quantitation (LLOQs) were 5 ng/ml for the total RO4929097 in plasma and 0.5 ng/ml for the unbound drug in phosphate buffer solution (PBS). Calibration curves were linear over RO4929097 concentration range of 5–2000 ng/ml in plasma for the total drug and 0.5–200 ng/ml in PBS for the unbound drug. The intra-day and inter-day accuracy and precision were within the generally accepted criteria for bioanalytical method (<15%). The method has been successfully employed to characterize the total and unbound plasma pharmacokinetics of RO4929097 after its oral administration in cancer patients.

© 2011 Elsevier B.V. All rights reserved.

## 1. Introduction

The Notch pathway is one major developmental signaling pathway that functions to maintain progenitor cells in a pluripotent state by regulating cell differentiation, proliferation, and survival [1]. It has been shown that Notch signaling is critical for the maintenance of tumor stem cells as well as maintenance of tumor cells in a less differentiated, highly proliferative state [2,3]. In mammalian cells, there are four Notch receptors (named Notch-1, -2, -3, and -4) and five ligands (named Jagged-1 and -2, and Deltalike (Dll)-1, -3 and -4) [4]. Notch signaling is initiated by receptor–ligand interactions between neighboring cells, resulting in a series of intramembrane cleavages, the last of which is mediated by the  $\gamma$ -secretase–presenilin complex [5]. The  $\gamma$ -secretase processing of Notch results in the release of the intracellular fragment of Notch (ICN), a functionally active form of Notch, which translocates to the nucleus and binds a DNA-binding protein, CBF-1 (CCAAT-binding factor 1). Notch–CBF-1 interactions directly alter the expression of key proliferation- and differentiation-specific genes [5]. Blocking

Notch signaling via  $\gamma$ -secretase inhibition is an attractive strategy to target tumor cells, tumor stem cells, and tumor endothelial cells.

RO4929097 is an orally bioavailable small-molecule inhibitor of  $\gamma$ -secretase, a key enzyme in the intramembrane proteolytic processing of several signaling receptors, including the Notch, amyloid precursor protein (APP), CD44, and Her4. In cell-free and cellular assays, RO4929097 inhibits  $\gamma$ -secretase with the IC<sub>50</sub> in low nanomolar range [6]. In tumor cells, RO4929097 inhibits Notch signaling, and it produces a less transformed, flattened, slower-growing phenotype [6]. RO4929097 shows antitumor activity in several xenografts models of different tumor types including colon, pancreatic, and non-small cell lung cancer [6].

RO4929097 is currently being evaluated in combination with GDC-0449 (a Hedgehog inhibitor) in patients with advanced breast cancer in a multi-center phase I study, with the Karmanos Cancer Institute being the lead institution (HIC #085709PH1F). Since the unbound drug concentration is believed to be a more reliable indicator of the target (intracellular) concentration and thus be more relevant of pharmacological and toxicological responses than the total drug, the plasma pharmacokinetics of the unbound as well as the total RO4929097 are examined in this phase I study. The unbound fraction of RO4929097 in patient plasma is determined using a semi-high throughput equilibrium dialysis method with 96-well microdialysis plates, as described previously [7]. In the present report, we described a specific, sensitive, accurate, and

\* Corresponding author at: Karmanos Cancer Institute, 4100 John R Street, HWCRC, Room 523, Detroit, MI 48201, USA. Tel.: +1 313 576 8258; fax: +1 313 576 8928.

E-mail address: [lijin@karmanos.org](mailto:lijin@karmanos.org) (J. Li).

reproducible method with high-performance liquid chromatography/tandem mass spectrometry (LC–MS/MS) for quantitation of the total RO4929097 in human plasma and the unbound drug in the post-dialysis buffer solution. The method was successfully applied for pharmacokinetic assessment of the total and unbound RO4929097 in cancer patients.

## 2. Experimental

### 2.1. Chemicals and reagents

RO4929097 and the internal standard D6-RO4929097 were provided by the Cancer Therapy Evaluation Program (CTEP), National Cancer Institute. All other chemicals and reagents were HPLC grade. Water was filtered and deionized with a US Filter PureLab Plus UV/UF system (Siemens, Detroit, MI, USA) and used throughout in all aqueous solutions. Drug-free (blank) human plasma from six different healthy donors was obtained from Innovative Research Inc. (Novi, MI, USA).

### 2.2. Stock solutions, calibration standards, and quality control samples

Stock solutions of RO4929097 and internal standard D6-RO4929097 were prepared in methanol at a concentration of 1 mg/ml, and stored in brown glass vials at  $-20^{\circ}\text{C}$ . Working stock solutions were prepared freshly on each day of analysis as serial dilutions in methanol. Two sets of calibration curve standards and quality control (QC) samples were prepared in blank human plasma and 10 mM phosphate buffer solution (PBS) (pH 7.2), respectively, for quantitation of the total RO4929097 in plasma and the unbound drug in the post-dialysis buffer solution. For the total drug, the calibration standards were prepared by spiking RO4929097 in blank human plasma at the concentrations of 5, 20, 50, 100, 200, 500, 1000 and 2000 ng/ml; the QC samples were prepared in blank plasma at the concentrations of 5 (lower limit of quantitation, LLOQ), 15, 80, and 1600 ng/ml. For the unbound drug, the calibration standards were prepared in PBS at the concentrations of 0.5, 2, 5, 10, 20, 50, 100, and 200 ng/ml; the QC samples were prepared in PBS at the concentrations of 0.5 ng/ml (LLOQ), 1.5, 80, and 160 ng/ml. All standards and QC samples were prepared fresh daily. For long-term and freeze–thaw stability, QC samples were prepared as a batch and stored at  $-80^{\circ}\text{C}$ .

### 2.3. Sample preparation

Frozen samples were thawed at ambient temperature. A 150  $\mu\text{l}$  aliquot of plasma sample (for the total drug) or PBS sample (for the unbound drug) was added into a 1.5-ml polypropylene eppendorf tube followed by spiking with 1 ml of ethyl acetate containing the internal standard D6-RO4929097 at the concentration of 40 ng/ml. The mixture was vortex-mixed for approximate 1 min, and centrifuged at 14,000 rpm for 5 min at ambient temperature. The top layer was transferred to a 1.5-ml polypropylene screw top tube, and evaporated to dryness under a stream of nitrogen in a water bath at  $40 \pm 5^{\circ}\text{C}$ . An aliquot of 100  $\mu\text{l}$  of reconstitution solution (methanol/0.45% formic acid in water, 60:40, v/v) was added into the tube. The mixture was vortex-mixed for 30 s followed by sonication for another 30 s and centrifuged at 14,000 rpm for 5 min. The supernatant was transferred to an autosampler vial, and 10  $\mu\text{l}$  was injected into the HPLC instrument using a temperature-controlled autosampling device (set at  $4^{\circ}\text{C}$ ).

### 2.4. Chromatographic and mass-spectrometric conditions

Chromatographic analysis was performed using a Waters Model 2695 HPLC system (Milford, MA, USA). Separation was achieved at  $30^{\circ}\text{C}$  using a Waters XTerra MS C<sub>18</sub> column (3.5  $\mu\text{m}$ ,  $50 \times 2.1$  mm i.d.) with a Waters XTerra RP<sub>18</sub> guard column (3.5  $\mu\text{m}$ ,  $10 \times 2.1$  mm i.d.). The mobile phase was composed of methanol–0.45% formic acid in water (60:40, v/v), and was pumped in isocratic model at the flow rate of 0.2 ml/min. The column effluent was monitored using a Waters Quattro Micro™ triple quadrupole mass spectrometry (Milford, MA, USA). The instrument was equipped with an electrospray ionization source, and controlled by the Masslynx 4.1 software. The analytes were detected in MRM mode using the positive ionization mode:  $m/z$  470.2 > 152.0 and 470.2 > 180.0 for RO4929097 in plasma and PBS samples, respectively;  $m/z$  476.2 > 196.0 for D6-RO4929097. The MS/MS conditions were as follows: capillary voltage, 3 kV; cone voltage, 26 V for RO4929097 and 20 V for D6-RO4929097; source temperature,  $120^{\circ}\text{C}$ ; desolvation temperature,  $350^{\circ}\text{C}$ ; desolvation gas flow, 500 l/h; collision energy, 90 and 27 eV for RO4929097 in plasma samples and PBS samples, respectively, and 40 eV for D6-RO4929097. Argon was used as collision gas at a pressure of 0.00463 mBar, and the dwell time per channel was 0.5 s for data collection.

### 2.5. Method validation

#### 2.5.1. Specificity and selectivity

The presence of endogenous interfering peaks was inspected by comparing the chromatograms of the extracted blank matrix (i.e., plasma from 6 donors or PBS) and those spiked with RO4929097 at the LLOQ (5 ng/ml in plasma and 0.5 ng/ml in PBS) and the internal standard (266 ng/ml). The interfering peak area should be less than 10% of the peak area for the analyte at the LLOQ and less than 5% of the peak area for the internal standard.

#### 2.5.2. Calibration curve, accuracy, and precision

Linearity was assessed at RO4929097 concentration ranging from 5 to 2000 ng/ml in plasma and 0.5 to 200 ng/ml in PBS. Calibration curves were built by fitting the analyte concentrations of the calibrators versus the peak area ratios of the analyte to internal standard using least-squares non-linear regression analysis with different weighting scheme (i.e., 1,  $1/x$ , and  $1/x^2$ ). The selection of weighting scheme was guided by evaluation of goodness-of-fit criteria including correlation coefficient ( $R^2$ ), deviations of the back-calculated concentrations, residual plots.

The intra- and inter-day accuracy and precision were assessed for the calibrator standards (each in duplicate) and QCs (including LLOQ, low, medium, and high QCs, each in quintuplicate) on three days. The accuracy was assessed as the relative percentage of the determined concentration to nominal concentration. The intra- and inter-day precisions were estimated by one-way analysis of variance (ANOVA) using the JMP™ statistical discovery software version 5 (SAS Institute, Cary, NC, USA). The inter-day variance ( $\text{VAR}_{\text{inter}}$ ), the intra-day variance ( $\text{VAR}_{\text{intra}}$ ), and the grand mean (GM) of the observed concentrations across runs were calculated from ANOVA analysis. The intra-day precision ( $P_{\text{intra}}$ ) was calculated as:

$$P_{\text{intra}} = 100 \times \left( \frac{\sqrt{\text{VAR}_{\text{intra}}}}{\text{GM}} \right)$$

The inter-day precision ( $P_{\text{inter}}$ ) was defined as:

$$P_{\text{inter}} = 100 \times \left( \frac{\sqrt{(\text{VAR}_{\text{inter}} - \text{VAR}_{\text{intra}})/n}}{\text{GM}} \right)$$

where  $n$  represents the number of replicate observations within each day.

### 2.5.3. Matrix effect and recovery

Matrix effect and recovery were assessed in human plasma (from 6 different donors) and in PBS, as described previously with modifications [8]. Three sets of QC samples (including low, medium and high QCs) were prepared. Set 1 QCs were prepared by spiking RO4929097 (at the low, medium, and high QC concentrations) and D6-RO4929097 in the matrix (i.e., human plasma or PBS) prior to extraction. After extraction, the analytes were reconstituted in a 100- $\mu$ l aliquot of the mobile phase for injection. Set 2 QCs was prepared by spiking the same amount of RO4929097 or D6-RO4929097 as Set 1 in a 100- $\mu$ l aliquot of blank matrix extracts (i.e., post-extraction reconstitution solution of blank plasma or PBS). Set 3 QCs was prepared by spiking the same amount of RO4929097 or D6-RO4929097 as Set 1 in a 100- $\mu$ l aliquot of the mobile phase to evaluate the detector response. The matrix effect is expressed as the ratio of the mean peak area of an analyte spiked post-extraction (set 2) to that from neat solution (set 3). The recovery is calculated as the ratio of the mean peak area of an analyte spiked prior to extraction (set 1) to that from post-extraction solution (set 2).

### 2.5.4. Stability

The short-term (bench-top) stability of the RO4929097 in methanol (working solution) at the concentration of 100 and 1  $\mu$ g/ml as well as in plasma at the concentration of 15 and 1600 ng/ml were tested at ambient temperature (25 °C) for 6 h. The stability of RO4929097 in plasma at the concentration of 15 and 1600 ng/ml were tested at 37 °C for 2, 4, 6, and 24 h. The autosampler stability of the analyte in the reconstitution solution (methanol/0.45% formic acid in water, 60:40, v/v) was examined at 4 °C for 12 h after the low and high QC plasma samples (at the concentration of 15 and 1600 ng/ml) were processed. The freeze–thaw stability of the RO4929097 in plasma at the concentrations of 15 and 1600 ng/ml was assessed through three freeze–thaw cycles. The long-term stability of RO4929097 in stock solution (1 mg/ml) and in plasma (15 and 1600 ng/ml) was investigated up to 8 and 7 months so far, respectively. All QCs were run in triplicate.

### 2.6. Application of the method to clinical pharmacokinetic study

Four patients participating in a phase I trial (NCI study #8420) at the Karmanos Cancer Institute received RO4929097 20 mg orally once daily on a 3-day on/4-day off schedule concurrently with oral GDC-0449 150 mg once daily. RO4929097 was administered once as a single agent orally on Day 1 to allow for single-agent pharmacokinetic sampling. GDC-0449 was administered as a single agent orally beginning on Day 8 and was given on a continuous daily schedule as monotherapy for two weeks. Starting Day 22 (Cycle 2, Day 1), GDC-0449 was administered orally daily, and RO4929097 was administered on days 1–3, 8–10 every 21 days (i.e., 3-day on/4-day off schedule). To examine the pharmacokinetics of RO4929097 when given alone, blood samples were collected in heparinized tubes at pre-dose, 0.5, 1, 1.5, 2, 3, 4, 8, 24, and 48 h after administration of the first dose of RO4929097. The protocol was approved by the Institutional Review Board of the Karmanos Cancer Institute at Wayne State University (Detroit, MI). All the patients provided written informed consent.

The blood sample was centrifuged at 4 °C, at 3000 rpm for 10 min, and plasma was collected and stored at –80 °C until analysis. The total concentrations of RO4929097 in patient plasma samples were determined using the described validated method. The unbound fraction of RO4929097 was obtained using equilibrium dialysis on a 96-Well Equilibrium DIALYZER™ with a 5-kDa

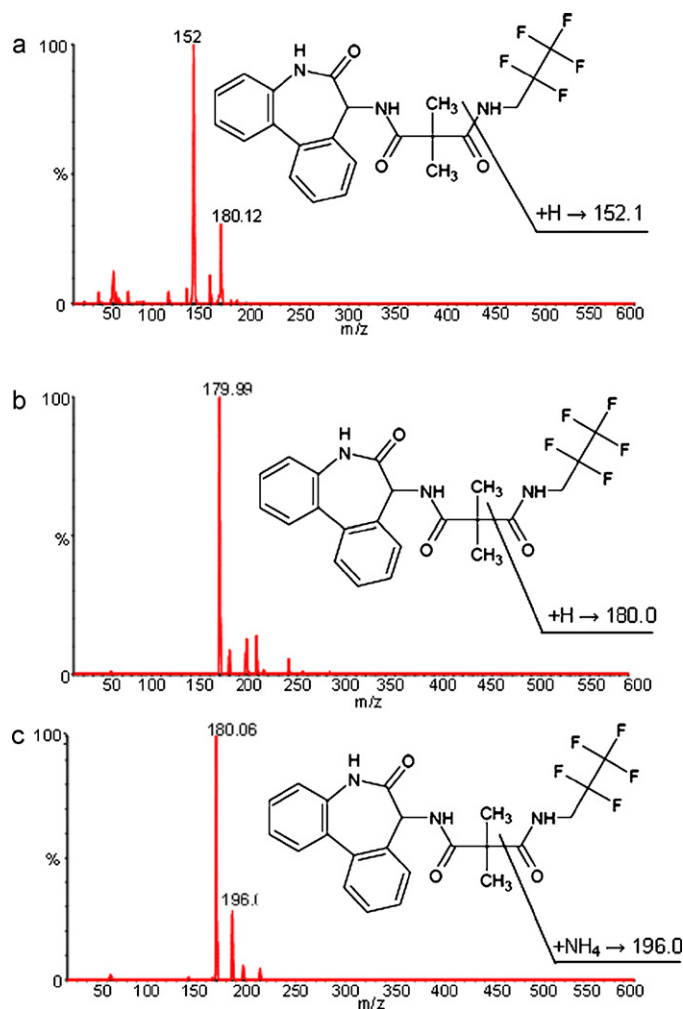


Fig. 1. Product mass spectrum of RO4929097 at  $m/z$  470.2  $\rightarrow$  152.0 used for plasma sample (a) and at  $m/z$  470.2  $\rightarrow$  180.0 used for PBS sample (b), and of the internal standard D6-RO4929097 at  $m/z$  476.2  $\rightarrow$  196.0 (c).

cut-off regenerated cellulose membrane (Harvard Apparatus Holliston, MA) [7]. Briefly, equilibrium dialysis was conducted with a 200- $\mu$ l aliquot of plasma against an equal volume of PBS (pH 7.2) at 37 °C for 24 h. The unbound concentration of RO4929097 in the post-dialysis buffer solution was determined using the present LC–MS/MS method. The pharmacokinetic parameters for the total and unbound RO4929097 were estimated using noncompartmental analysis with the computer software program WinNonlin 5.2 (Pharsight Corporation, Mountain View, CA).

## 3. Results and discussion

### 3.1. LC–MS/MS spectrometry and specificity

In the positive ion mode, RO4929097 and D6-RO4929097 showed protonated molecule ions ( $MH^+$ ) at  $m/z$  470.2 and 476.2, respectively. RO4929097 produced a most abundant product ion at  $m/z$  180.0 under the collision energy of 27 eV. However, there was an interfering peak from blank human plasma when RO4929097 was monitored at  $m/z$  470.2  $>$  180.0. Therefore, a less but still sensitive transition  $m/z$  470.2  $\rightarrow$  152.0 was selected for the detection of the total RO4929097 in plasma samples (Fig. 1a), while the most sensitive  $m/z$  470.2  $>$  180.0 was used for the detection of unbound RO4929097 in PBS samples because there was

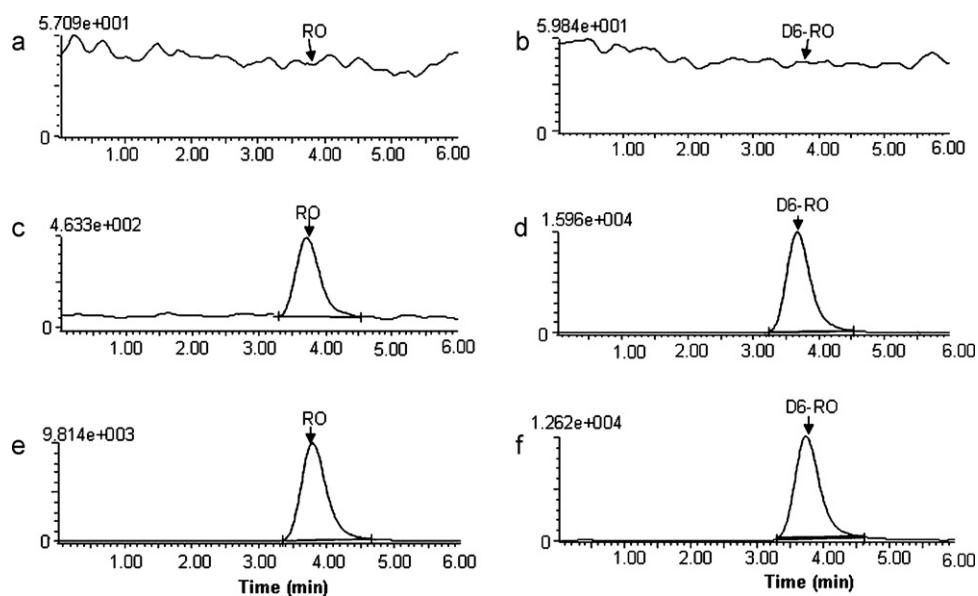


**Fig. 2.** Chromatograms of blank plasma (a and b), spiked plasma with RO4929097 at LLOQ (5 ng/ml) (c and d), and a patient plasma sample collected at 2.0 h after oral administration of a single dose of RO4929097 (20 mg) (e and f), monitored at  $m/z$  470.2  $\rightarrow$  152.0 for RO4929097 and at  $m/z$  476.2  $\rightarrow$  196.0 for D6-RO4929097. The retention times for RO4929097 and D6-RO4929097 were  $3.8 \pm 0.01$  and  $3.7 \pm 0.02$  min, respectively.

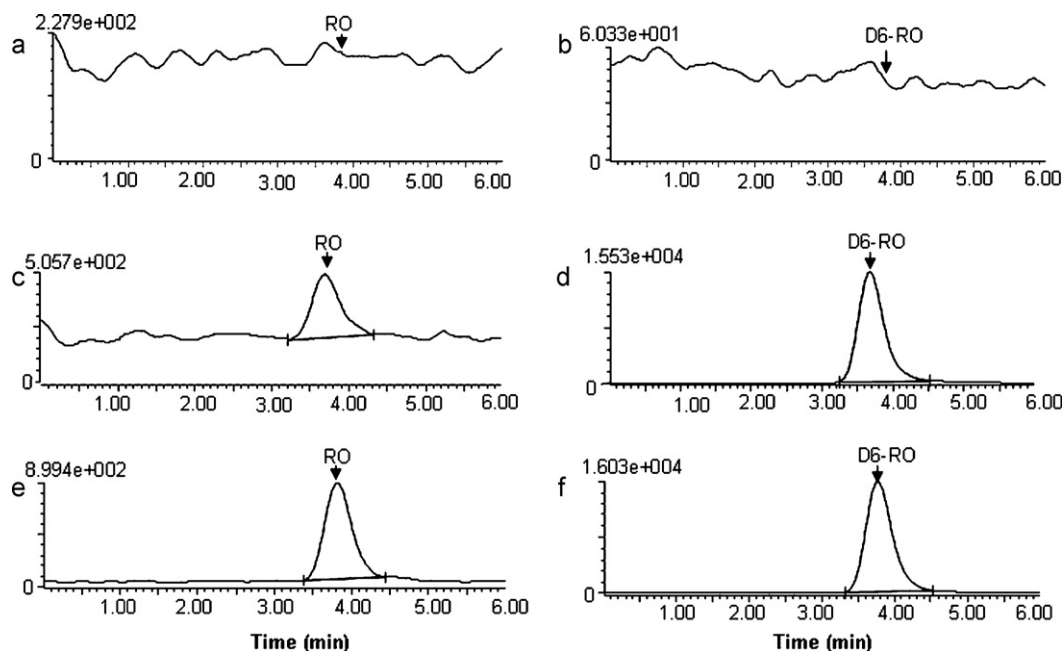
no interference from PBS at this transition (Fig. 1b). The internal standard, D6-RO4929097 was monitored at  $m/z$  476.2  $>$  196.0 (Fig. 1c).

Fig. 2 shows the representative chromatograms of the blank human plasma and plasma spiked with RO4929097 (at the LLOQ of 5 ng/ml) and D6-RO4929097 (at 266 ng/ml) as well as a patient plasma sample collected at 2 h after the oral administration of RO4929097 20 mg. Fig. 3 shows the representative chromatograms of the blank PBS and PBS spiked with RO4929097 (at the LLOQ of 0.5 ng/ml) and D6-RO4929097 (at 266 ng/ml) as well as the post-dialysis buffer solution sample from a patient plasma sample collected at 2 h after the oral administration of RO4929097 20 mg. The mean ( $\pm$  standard deviation) retention

times for RO4929097 and D6-RO4929097 were at  $3.76 \pm 0.02$  and  $3.74 \pm 0.02$  min, respectively, with an overall chromatographic run time of 6 min. Blank plasma samples from 6 different donors as well as pre-treatment plasma samples from the patients showed no interference for the analyte and internal standard.

### 3.2. Linearity, accuracy, and precision

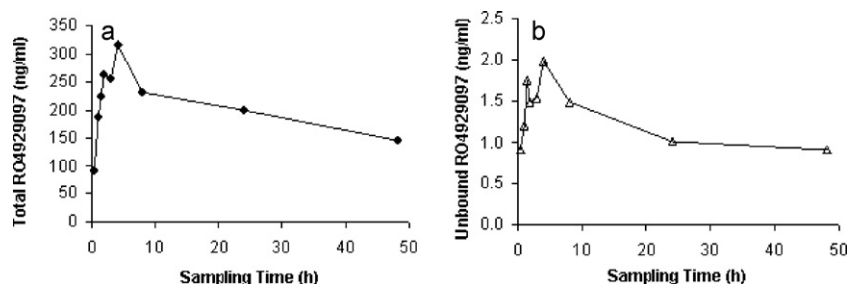
The linear calibration curves were established over the range of 5–2000 ng/ml and of 0.5–200 ng/ml for the total RO4929097 in plasma and the unbound drug in PBS, respectively. The relationship between peak area ratios of the analyte to internal standard versus the analyte concentrations was best fitted by a linear



**Fig. 3.** Chromatograms of blank PBS (a and b), spiked PBS with RO4929097 at LLOQ (0.5 ng/ml) (c and d), and the post-dialysis buffer solution from a patient plasma sample collected at 2.0 h after oral administration of a single dose of RO4929097 (20 mg) (e and f), monitored at  $m/z$  470.2  $\rightarrow$  180.0 for RO4929097 and at  $m/z$  476.2  $\rightarrow$  196.0 for D6-RO4929097. The retention times for RO4929097 and D6-RO4929097 were  $3.8 \pm 0.01$  and  $3.7 \pm 0.02$  min, respectively.

**Table 1**Accuracy, intra- and inter-day precisions of calibrator standards<sup>a</sup> of the calibration curves of RO4929097 in plasma and in phosphate buffer solution (PBS, pH 7.2).

Matrix	Nominal concentration (ng/ml)	Determined concentration (mean ± SD) (ng/ml)	Average accuracy (%)	Intra-day (%)	Inter-day (%)
Human plasma	5 (LLOQ)	5.1 ± 0.3	101	5.2	– <sup>b</sup>
	20	20.7 ± 1.2	104	4.3	3.9
	50	51.7 ± 1.7	103	3.5	– <sup>b</sup>
	100	100.9 ± 3.1	101	3.8	– <sup>b</sup>
	200	201.4 ± 4.8	101	2.8	– <sup>b</sup>
	500	485.7 ± 10.6	97	2.8	– <sup>b</sup>
	1000	981.2 ± 51.2	98	6.0	– <sup>b</sup>
	2000	1963.6 ± 72.5	98	4.6	– <sup>b</sup>
PBS (pH 7.2)	0.5 (LLOQ)	0.48 ± 0.04	97	8.4	– <sup>b</sup>
	2	2.00 ± 0.03	102	4.0	4.9
	5	5.1 ± 0.1	101	2.0	2.1
	10	10.1 ± 0.4	101	5.1	– <sup>b</sup>
	20	21.0 ± 2.1	105	9.9	2.4
	50	49.9 ± 1.2	100	3.1	– <sup>b</sup>
	100	98.8 ± 1.4	99	1.4	– <sup>b</sup>
	200	194.5 ± 4.3	97	1.9	1.3

<sup>a</sup> Each calibrator standard was evaluated in duplicate on three different days.<sup>b</sup> No additional variation was observed as a result of performing assay in different days.**Fig. 4.** Mean plasma concentration–time profiles of the total (a) and unbound (b) RO4929097 after oral administration of the first single dose of RO4929097 20 mg to four patients with advanced breast cancer.

equation, expressed as  $y = a \cdot x + b$ , where  $y$  is peak area ratio,  $x$  is the analyte concentration,  $a$  and  $b$  are fitted parameters. A weighting function of  $1/x^2$  produced the best goodness-of-fit. A linear correlation coefficient ( $R$ ) of  $>0.99$  was obtained in all analytical runs.

The LLOQ for RO4929097 was established at 5 ng/ml for plasma samples and 0.5 ng/ml for PBS samples, at which the mean signal-to-noise ratios were  $30 \pm 10$  ( $n = 15$ ) and  $31 \pm 14$  ( $n = 15$ ), respectively. For all calibrator standards (including LLOQ) of RO4929097 in either plasma or PBS, the average accuracy in terms of the percentage of the back-calculated concentrations relative to the nominal concentrations ranged from 97% to 105%; the intra-day and inter-day precisions were less than 9.9% (Table 1).

The intra- and inter-day accuracy and precision were assessed for RO4929097 at the LLOQ and at the low, medium, and high QC concentrations in both plasma and PBS samples over 3 days. For the QCs of RO4929097 in plasma at 5 ng/ml (LLOQ), 15, 800, and 1600 ng/ml, the average accuracy ranged from 96% to 100%;

the intra- and inter-day precisions were within 7.6% (Table 2). For the QCs of RO4929097 in PBS at 0.5 ng/ml (LLOQ), 1.5, 80, and 160 ng/ml, the average accuracy ranged from 97% to 100%; the intra- and inter-day precisions were within 11.1% (Table 2).

### 3.3. Matrix effect and recovery

The matrix effect was examined in 6 different sources of human plasma and in PBS to assess the possibility of ionization suppression or enhancement for RO4929097 and the internal standard D6-RO4929097. The average plasma matrix effects from 6 different sources of plasma were determined ranging from 104% to 119% for RO4929097 (at 15, 800, and 1600 ng/ml) and D6-RO4929097 (at 100 ng/ml) (Table 3). The variability in plasma matrix effect, as measured by the coefficient of variation (CV%) from 6 different sources of plasma, was less than 3.3% (Table 3). The PBS matrix effects for RO4929097 (at 1.5, 80, and 160 ng/ml) and D6-RO4929097 (at 100 ng/ml) were less than 101% (Table 3). The results suggest that

**Table 2**Accuracy, intra- and inter-day precisions for the QC samples<sup>a</sup> of RO4929097 in human plasma and in phosphate buffer solution (PBS, pH 7.2).

Matrix	Nominal concentration (ng/ml)	Determined concentration (mean ± SD) (ng/ml)	Average accuracy (%)	Intra-day (%)	Inter-day (%)
Human plasma	5 (LLOQ)	4.8 ± 0.4	96	7.6	2.7
	15	15.0 ± 0.9	100	5.9	– <sup>b</sup>
	800	776.2 ± 26.6	97	2.9	2.2
	1600	1582.0 ± 47.7	99	3.0	– <sup>b</sup>
PBS (pH 7.2)	0.5 (LLOQ)	0.49 ± 0.06	97	11.1	8.2
	1.5	1.50 ± 0.10	100	7.1	– <sup>b</sup>
	80	79.3 ± 1.1	99	1.3	0.7
	160	156.9 ± 3.6	98	2.2	0.4

<sup>a</sup> Each QC was performed in quintuplicate on three different days.

**Table 3**  
Matrix effect and recovery of RO4929097 and the internal standard D6-RO4929097 from 6 different sources of human plasma and from phosphate buffer solution (PBS, pH 7.2).

Matrix	Analyte	Nominal concentration (ng/ml) <sup>a</sup>	Mean peak area			Matrix effect (%) <sup>e</sup>	Recovery (%) <sup>f</sup>
			Set 1 <sup>b</sup>	Set 2 <sup>c</sup>	Set 3 <sup>d</sup>		
Human plasma	RO4929097	15	1616	1818	1548	117 (2.5%)	89 (9.0%)
		800	73,806	87,629	87,075	104 (3.0%)	84 (5.1%)
		1600	169,103	214,875	181,157	119 (1.8%)	79 (3.7%)
PBS	D6-RO4929097	100	10,876	13,812	11,774	117 (3.3%)	79 (7.4%)
		RO4929097	1.5	765	973	1049	93 (7.6%)
	D6-RO4929097	80	35,172	37,314	36,839	101 (0.8%)	94 (0.9%)
		160	70,768	75,336	75,631	99 (0.5%)	94 (0.3%)
		100	7244	7852	7835	99 (6.0%)	98 (7.1%)

<sup>a</sup> The nominal concentrations of the analyte spiked in plasma before extraction (set 1). The same amounts of the analyte as in set 1 were spiked in the mobile phase and in plasma or PBS extract for set 3 and set 2.

<sup>b</sup> The mean peak area of an analyte that was spiked before extraction in plasma from 6 different sources (donors), each source of plasma in triplicate measurements.

<sup>c</sup> The mean peak area of an analyte that was spiked postextraction in plasma extracts from 6 different sources of human plasma, each source of plasma in triplicate measurements.

<sup>d</sup> The mean peak area of an analyte that was spiked in the mobile phase from triplicate measurements.

<sup>e</sup> Matrix effect is expressed as the ratio of the mean peak area of an analyte spiked postextraction (set 2) to the mean peak area of the same amount of analyte spiked in the mobile phase (set 3). Data are shown as the mean (%CV) from six different sources of plasma.

<sup>f</sup> Extraction recovery is calculated as the ratio of the mean peak area of an analyte spiked before extraction (set 1) to the mean peak area of the same amount of the analyte spiked postextraction (set 2). Data are shown as the mean (%CV) from six different source of plasma.

there is no significant ionization suppression or enhancement from the matrix (i.e., different sources of human plasma or PBS) for the analyte and internal standard.

The recovery need not be very high, but it should be consistent and reproducible [9]. The average recovery for RO4929097 (at 15, 800, and 1600 ng/ml) and D6-RO4929097 (at 100 ng/ml) from 6 different sources of human plasma ranged from 79% to 89%; the variability in recovery, as assessed by the CV% from the 6 different sources of plasma was within 9.0% (Table 3). For RO4929097 and D6-RO4929097 in PBS samples, the recovery ranged from 79% to 98% (Table 3). All these data suggested that the extraction recoveries from either plasma or PBS were consistent and reproducible for the analyte and internal standard.

### 3.4. Stability

The short- and long-term stabilities of RO4929097 were demonstrated in Table 4. Bench-top stability test suggested that RO4929097 was stable in both methanol (at 1 and 100 µg/ml) and human plasma (at 15 and 1600 ng/ml) at ambient temperature (~25 °C) for at least 6 h. RO4929097 was stable in human plasma (at 15 and 1600 ng/ml) at 37 °C for at least 24 h, allowing equilibrium dialysis to perform at 37 °C for at least 24 h. Autosampler stability test suggested that RO4929097 was stable in the reconstitution solution (methanol/0.45% formic acid in water, 60:40, v/v) at 4 °C for at least 12 h, allowing the assay to be performed continuously overnight for a large number of samples. Freeze–thaw stability test suggested that RO4929097 at the concentrations of 15 and 1600 ng/ml in human plasma showed less than 4% degradation through three full cycles of freeze–thaws. The long-term stability tests suggested that RO4929097 was stable in methanol at 1 mg/ml (stock solution) at –20 °C for at least eight months. It was stable in human plasma (at 15 and 1600 ng/ml) at –80 °C for 3 months (Table 4). The long-term stability for RO4929097 stock solution –20 °C are continuously monitored.

### 3.5. Clinical application

The present LC–MS/MS method was successfully employed to study the plasma pharmacokinetics of the total and unbound RO4929097 in four patients with advanced breast cancer. Fig. 4 shows the mean plasma concentration–time profiles of the total and unbound RO4929097 after oral administration of the first

single dose of RO4929097 20 mg to four patients. After an oral dose of RO4929097 20 mg, the mean observed maximum plasma concentrations ( $C_{max}$ ) of the total and unbound RO4929097 were 332 ng/ml (range, 72–657 ng/ml) and 2.3 ng/ml (range, 1.7–2.7 ng/ml), respectively; the mean values of the area under the curve to the last sampling time point ( $AUC_{0-48h}$ ) for the total and unbound drug were 8755 ng/ml × h (range, 899–18928 ng/ml × h) and 50 ng/ml × h (range, 16–86 ng/ml × h), respectively. The fraction unbound of RO4929097 varied from 0.2% to 3%, with a mean value of 1.0%, after oral administration of a single dose of RO4929097 20 mg to four patients.

**Table 4**  
Assessment of stability of RO4929097.

	RO4929097 concentration (ng/ml) <sup>c</sup>	
	15	1600
Bench-top stability (in plasma) (25 °C) (%) <sup>b</sup>		
1.0 h	98	98
2.0 h	107	107
3.0 h	99	105
4.0 h	98	106
6.0 h	103	106
Stability in plasma at 37 °C (%) <sup>b</sup>		
2.0 h	91	94
4.0 h	93	97
6.0 h	95	100
24.0 h	93	101
Auto-sampler stability (in the mobile phase) (4 °C) (%) <sup>a</sup>		
1.0 h	100	99
2.0 h	98	100
4.0 h	98	98
8.0 h	96	98
12.0 h	96	97
Freeze–thaw stability (in plasma) (–80 °C) (%) <sup>b</sup>		
Cycle 1	100	102
Cycle 2	99	96
Cycle 3	98	97
Long-term stability (in plasma) (–80 °C) (%) <sup>b</sup>		
1.5-month	102	108
3.0-month	90	93
7.0-month	76	79

<sup>a</sup> Stability data is expressed as the mean percentage of the peak area determined at certain time relative to that at time zero.

<sup>b</sup> Stability data is expressed as the mean percentage of the analyte concentration determined at certain time point relative to the nominal concentration (%).

<sup>c</sup> Each concentration at each time point was assessed in triplicate.

#### 4. Conclusion

A sensitive and reliable LC–MS/MS method has been developed and validated for quantitation of the total and unbound RO4929097 in human plasma. The LLOQ was 5 ng/ml for the total RO4929097 in plasma and 0.5 ng/ml for the unbound drug in PBS. Linear calibration curves were established over the concentration range of 5–2000 ng/ml in plasma for the total RO4929097 and 0.5–200 ng/ml in PBS for the unbound drug. The method has been successfully applied to the study of the total and unbound plasma pharmacokinetics of RO4929097 after its oral administration in patients with advanced breast cancer in a phase I clinical trial.

#### Acknowledgments

This study was supported by the United States Public Health Service Cancer Center Support Grant P30 CA022453 and the National Institute of Health grant U01 CA062487.

#### References

- [1] S. Artavanis-Tsakonas, M.D. Rand, R.J. Lake, *Science* 284 (1999) 770.
- [2] A. Telerman, R. Amson, *Nat. Rev. Cancer* 9 (2009) 206.
- [3] P. Rizzo, C. Osipo, K. Foreman, T. Golde, B. Osborne, L. Miele, *Oncogene* 27 (2008) 5124.
- [4] A. Baldi, M. De Falco, L. De Luca, G. Cottone, M.G. Paggi, B.J. Nickoloff, L. Miele, A. De Luca, *Biol. Cell* 96 (2004) 303.
- [5] A.C. Tien, A. Rajan, H.J. Bellen, *J. Cell Biol.* 184 (2009) 621.
- [6] L. Luistro, W. He, M. Smith, K. Packman, M. Vilenchik, D. Carvajal, J. Roberts, J. Cai, W. Berkofsky-Fessler, H. Hilton, M. Linn, A. Flohr, R. Jakob-Rotne, H. Jacobsen, K. Glenn, D. Heimbrook, J.F. Boylan, *Cancer Res.* 69 (2009) 7672.
- [7] J. Li, J. Brahmer, W. Messersmith, M. Hidalgo, S.D. Baker, *Invest. New Drugs* 24 (2006) 291.
- [8] R. Wiegand, J. Wu, X. Sha, P. LoRusso, J. Li, *J. Chromatogr. B Analyt. Technol. Biomed. Life Sci.* 878 (2010) 333.
- [9] S. Bansal, A. DeStefano, *AAPS J.* 9 (2007) E109.